

Theoretical investigation of quantum capacitance in the functionalized MoS₂-monolayer

Sruthi T, Nayana Devaraj and Kartick Tarafder*

*Department of Physics, National Institute of Technology Karnataka,
Surathkal, PO: Srinivasnagar, Mangalore – 575025.*

(Dated: June 24, 2021)

In this work, we investigated the electronic structure and the quantum capacitance of the functionalized MoS₂ monolayer. The functionalizations have been done by using different ad-atom adsorption on MoS₂ monolayer. Density functional theory calculations are performed to obtain an accurate electronic structure of ad-atom doped MoS₂ monolayer with a varying degree of doping concentration. The quantum capacitance of the systems was subsequently estimated. A marked quantum capacitance above 200 $\mu\text{F}/\text{cm}^2$ has been observed. Our calculations show that the quantum capacitance of MoS₂ monolayer is significantly enhanced with substitutional doping of Mo with transition metal ad-atoms. The microscopic origin of such enhancement in quantum capacitance in this system has been analyzed. Our DFT-based calculation shows that generation of new electronic states at the proximity of the band-edge and the shift of Fermi level caused by the ad-atom adsorption results in a very high quantum capacitance in the system.

INTRODUCTION

The creation of adequate energy from sustainable energy sources, bypassing the utilization of fossil fuels, is one of the greatest challenges to stifle the weather change. Large-scale generation of green energy from sustainable power sources is, therefore, highly essential in the current situation. On the other hand, technology needs to be developed that can efficiently convert and store the generated energy. Batteries, fuel cells, and supercapacitors are the essential technological devices that help to convert and store energy. Of these, supercapacitors have received the most attention in recent times due to its high power density, long lifetime, good stability, and their possible applications over a wide temperature range [1, 2]. Supercapacitors can temporarily store a large amount of electrical energy and release it when needed. However, their low energy density and high production cost are a hindrance to their progress [3]. It is essential to overcome these drawbacks to expand the use of supercapacitors. Intense research is going on to overcome the obstacle - low energy density- by changing the electrode material of supercapacitors. The most commonly considered electrodes are carbon-based materials because of their high specific surface area, good electrical conductivity, and good stability [4, 5]. One of the essential requirements for a supercapacitor is the electrode material should possess a large specific area with significantly high ion density. Two-dimensional materials that are in general, possess a large specific area, therefore, could be the best alternative for supercapacitor electrode applications. Graphene, an atom-thick 2D material in which carbon atoms are arranged in a honeycomb lattice, has remarkable electrical and mechanical properties. It has been reported recently that graphene can also be used as

a suitable building block for supercapacitors [6]. Studies have been carried out by considering graphene, chemically modified graphene, and graphene-based composites as supercapacitor electrodes [7–10]. However, the poor scalability [11, 12] hinders its large scale application, which necessitated to search for other suitable two dimensional materials for supercapacitor electrodes. Transition metal dichalcogenides can take an active part in designing such materials. MoS₂ belongs to this class of materials is already well-known to the materials science community, has already been proven to be very suitable for applications in many fields including catalysis, lithium-ion batteries, phototransistors due to their unique morphology, excellent electrical and mechanical properties [13–16]. Bulk MoS₂ consists of S-Mo-S units, which are held together by weak van der Waals interactions [17]. Therefore, using physical or chemical methods, single or few layers of MoS₂ can be easily exfoliated from bulk MoS₂ [18, 19]. The excellent electrical and electrochemical properties, mechanical flexibility, versatile electronic states and good environmental characteristics of MoS₂ can also be used as a suitable candidate for supercapacitor electrode applications [20][21][22].

In 2007, Soon and Lohz investigated the double-layer electrochemical capacitance of nano-walled MoS₂ film using electrochemical impedance spectroscopy and have shown that edge-aligned MoS₂ thin films can act as a supercapacitor at various current frequencies, which can be compared to a carbon nanotube array electrode. They also have found that ion diffusion at slow scanning speeds results in Faradaic capacitance, which greatly improves the capacitance [23]. In 2013 Ma et.al reported a method to synthesize a polypyrrole/MoS₂(PPy/MoS₂) nano-composite as an innovative electrode material for efficient supercapacitors [24]. Another method adopted to develop better supercapacitors is to increase capacitance by doping of different atoms to the electrode materials. Xu et.al explored the change in quantum capacitance due to doping and co-doping on graphene-based

* karticktarafder@gmail.com

electrodes using first principle methods [25]. They have found that the N/S and N/P co-doped graphene with vacancy defects are suitable for asymmetric supercapacitors. In one of our previous work, we have observed very high quantum capacitance in the functionalized graphene modified with ad-atoms [26]. So it is clear from the available literature that with proper functionalization, MoS₂ can be made a suitable material for the super-capacitor electrode applications. Therefore, in this work, we have functionalized the MoS₂ with different ad-atoms to modify the quantum capacitance of supercapacitors having a monolayer MoS₂ electrode and investigated the microscopic origin of these changes.

METHODOLOGY

Structural optimization and subsequently the electronic structure information of different functionalized systems are obtained by using first-principle density functional theory calculations as implemented in the Vienna Ab-initio Simulation Package VASP[27, 28]. The Generalized-gradient approximation with the Perdew–Burke–Ernzerhof (PBE) parameterization was used to describe the exchange–correlation energy [29]. A very high value of the energy cut-off (>400eV) was taken into consideration to obtain accurate results. To study the impact of various ad-atom substitution on the quantum capacitance, calculations were done utilizing 3×3×1 supercells of MoS₂ unit cell, having nine Mo atoms and eighteen sulfur atoms. Single Mo or S atomic sites were selected for substitutional doping. The vacancy defected configurations were studied on the same supercell of MoS₂ with varying vacancy concentration [30]. A large void space (height>10Å) was considered along the out of the plane direction of layer MoS₂ unit cells to prevent the interaction with its periodic images. We have used a 6×6×1 Monkhorst-Pack grids to sample the Brillouin zone for geometrical optimization with 10⁻⁶ H total energy tolerance for convergence. A denser 24×24×1 Monkhorst-Pack grids were used for the precise extraction of electron density of states D(E) and atom projected density of states (PDOS).

The total capacitance, C_T of an electrical double-layer capacitor (EDLC) is expressed as

$$\frac{1}{C_T} = \frac{1}{C_Q} + \frac{1}{C_D} \quad (1)$$

where C_Q and C_D are quantum capacitance and double-layer capacitance. The quantum capacitance of materials is defined as the rate of variation of excessive charges (ions) over the change in applied potential [31]. So it is directly related to the electronic energy configuration of the electrode materials and can be defined as the derivative of the net excess charge on the substrate/electrode with respect to electrostatic potential. ie,

$$C_Q = \frac{dQ}{d\phi} \quad (2)$$

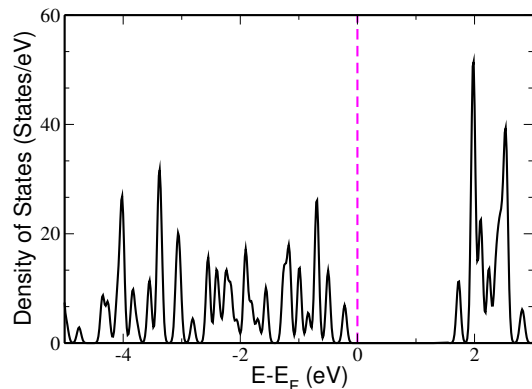


FIG. 1: (color online) Density of states of MoS₂. Vertical magenta dashed line is the Fermi energy set at $E=0$.

where Q is the excessive charge on the electrode and ϕ is the chemical potential. The total charge is in proportion to the weighted sum of the electronic DOS up to the Fermi level, E_F . Due to an applied potential, the chemical potential will be shifted, the excessive charge on the electrode (Q) then can be expressed by an integral term associated with the electronic density of state $D(E)$ and the Fermi-Dirac distribution function $f(E)$ as

$$Q = e \int_{-\infty}^{+\infty} D(E)[f(E) - f(E - \phi)]dE \quad (3)$$

Therefore, when the density of states (DOS) is known, the C_Q of a channel at a finite temperature T can be calculated as

$$C_Q = \frac{dQ}{d\phi} = \frac{e^2}{4kT} \int_{-\infty}^{+\infty} D(E) \text{sech}^2 \frac{E - e\phi}{2kT} dE \quad (4)$$

Here, ϕ , e , and k are chemical potential, charge of an electron, and the Boltzmann constant respectively.

RESULTS AND DISCUSSIONS

The equation (4) shows the role of the DOS present near the Fermi energy. Since the monolayer MoS₂ is a direct band semiconductor [32], in which no states are present near Fermi level (Fig.1), it gives zero quantum capacitance. The electronic structure of a material can be modified using ad-atom doping. If the change in electronic structure could accumulate states near Fermi level then the quantum capacitance can be generated in the monolayer MoS₂.

Substitutional doping effect of Monolayer MoS₂

The substitutional doping on MoS₂ can be done by selecting atoms from groups in the periodic table

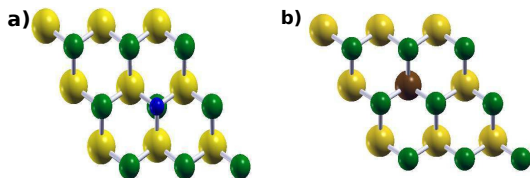


FIG. 2: (color online) Structure of functionalized MoS₂.

Green balls and yellow balls represent S and Mo respectively. a) Structure of S substituted MoS₂. Blue ball represent the atom which substitute S. b) Structure of Mo substituted MoS₂. Brown ball represent the atom which substitute Mo.

which are nearer to Mo and S atom. Hence we have investigated the change in quantum capacitance of MoS₂ by substituting S atoms with group five atoms as well as atoms from the halogen family. Whereas transition metal atoms are selected to replace the Mo atom. The geometric structure of the doped atoms is shown in Fig.2.

The Stability of doped MoS₂ structures has been examined by estimating average adsorption energy E_{ad} using the equation

$$E_{ad} = \frac{1}{n} [E_{tot} - E_{MoS_2} - nE_{at}] \quad (5)$$

where E_{tot} is the total energy of the functionalized MoS₂ unit cell, E_{MoS_2} is the total energy of pristine MoS₂ in the same unit cell, E_{at} is the per atom energy of the ad-atom and n represents the number of ad-atoms present in the unit cell. The adsorption energies for various functionalized MoS₂ are listed in the Table.I. Relatively large adsorption energies indicate that these atoms can be easily substituted on the pristine MoS₂ surface.

TABLE I: Adsorption energy per ad-atoms adsorbs on MoS₂ Monolayer.

ad-atom	adsorption energy(in eV)	ad-atom	adsorption energy(in eV)
N	-2.139	F	-2.039
As	-2.001	Cl	-0.272
Sb	-1.208	Cu	-1.953
Se	-2.091	Ni	-2.142

Substitution of Sulfur by ad-atoms of group-V and group-VII

We first investigated the effect of substitutional doping of sulfur in the MoS₂. N, As, Sb, and Se from the group-V, F, and Cl from group-VII are considered to replace on S atom in the unit cell. The atom projected density of states for S atom substituted with group-V ad-atoms are shown in Fig.3. Note that the accumulation of energy states from the substituted dopant atoms near the

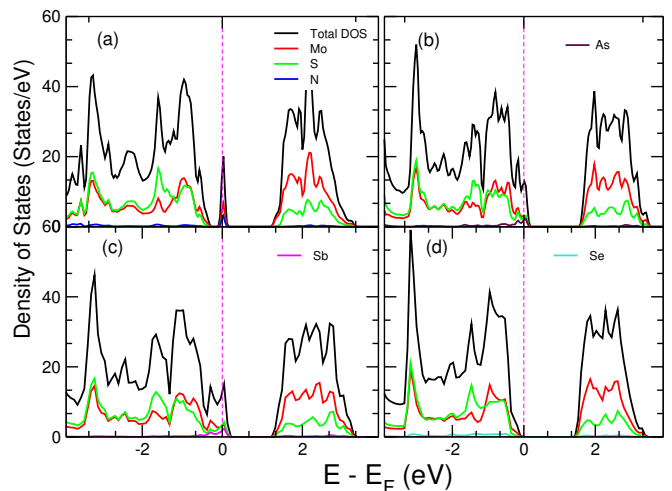


FIG. 3: (color online) Atom projected density of states for functionalized MoS₂ with (a)N, (b)As, (c)Sb and (d)Se atoms. Colored curve represents dos from the doped atom. Vertical magenta dashed line is the Fermi energy set at $E=0$.

Fermi level occurs in each case except Se doping. Since the quantum capacitance is directly proportional to the measure of DOS near the Fermi level, the quantum capacitance is expected to be changed in these systems. The calculated quantum capacitance of the functionalized MoS₂ for various group five ad-atom substitution for sulfur is shown in Table.II. Maximum quantum capacitance, 203 $\mu\text{F}/\text{cm}^2$ has been obtained for nitrogen substituted MoS₂ monolayer. Whereas no significant change in the electronic structure of MoS₂ as well as in quantum capacitance has been observed for Se doping.

TABLE II: Details of C_Q value calculated at Fermi energy for various ad-atom functionalized MoS₂ Monolayer.

Configuration	C_Q ($\mu\text{F}/\text{cm}^2$)	Configuration	C_Q ($\mu\text{F}/\text{cm}^2$)
FG - N	203.047	FG - Sb	188.955
FG - As	189.672	FG - Se	0.595

To analyze the result one should note that the N, As, and Sb substitution of S atom on MoS₂ monolayer leads to a hole doping condition where the Fermi-level comes close to the valence band. The electron deficiency in the system forces a charge redistribution in the presence of these three substituted ad-atom, which intern helps to accumulate a large amount of density of states near the valence band edge close to the Fermi energy. To confirm this situation we have calculated the charge density difference, associated with functionalized MoS₂ where the average charge density of MoS₂ was subtracted from the functionalized charge density. Fig.4 shows the resulted charge distribution upon substitutional doping of MoS₂ with N, As, Sb, and Se ad-atoms. The homogeneity of the

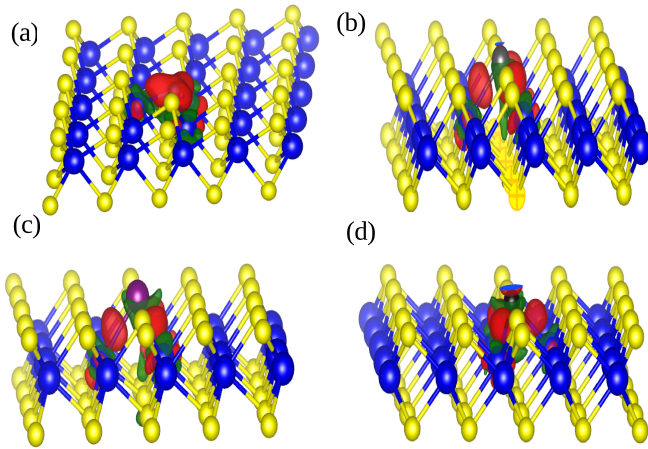


FIG. 4: (color online) Change in electron density associated with Functionalized MoS₂ Monolayer with (a)N, (b)As, (c)Sb and (d)Se doping. Red and green isosurface represents the charge accumulation and electron deficiency in the system. The blue and yellow balls represents Mo and S atoms in MoS₂ Monolayer.

charge distribution gets significantly disrupted because of the substituted ad-atoms, and charge accumulation near the Mo atom reflects the accumulation of DOS near the valence band edge of the functionalized systems.

In the case of group-VII ad-atoms such as F and Cl functionalization, the substitution of S with these atoms brings the electron doping situation in the system. Here the Fermi energy shifted close to the conduction band and one excess electron in the unit cell will also assist the charge redistribution in the system. Therefore these ad-atoms are capable of significant changes in the DOS as shown in Fig.5. A similar electron density difference plot for F and Cl doped system is shown in Fig.6 indicates that the electrons are accumulating near the doped site. Further, accumulation of large density of state near the conduction band has also been observed in the partial density of state plot shown in Fig.5.

Accumulation of DOS near the fermi energy enhanced the C_Q value of the functionalized systems. We have calculated $139 \mu\text{F}/\text{cm}^2$ and $252 \mu\text{F}/\text{cm}^2$ C_Q values for F and Cl functionalized systems respectively. The energy variation of C_Q in different ad-atom doped(replacement of a S atom) systems are shown in Fig.7

Substitution of Mo with Transition Metal(TM) ad-atoms

Next, we have considered transition metal atoms such as Co, Cu, Ni, and V as ad-atoms to substitute one Mo in the MoS₂ monolayer unit cell. The atom projected density of states (Fig.8) shows that Co, Cu, Ni, and V are also introduces DOS near Fermi energy. Our calculation shows a large change in the C_Q value of upon TM-functionalization of MoS₂ monolayers. The maximum

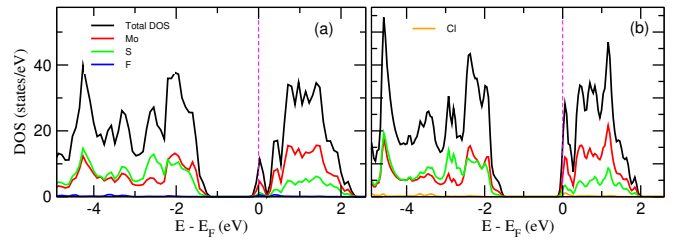


FIG. 5: (color online) Atom projected density of states for functionalized MoS₂ with (a)F and (b)Cl atoms. Colored curve represents dos from the doped atom. Vertical majenta dashed line is the Fermi energy set at $E=0$.

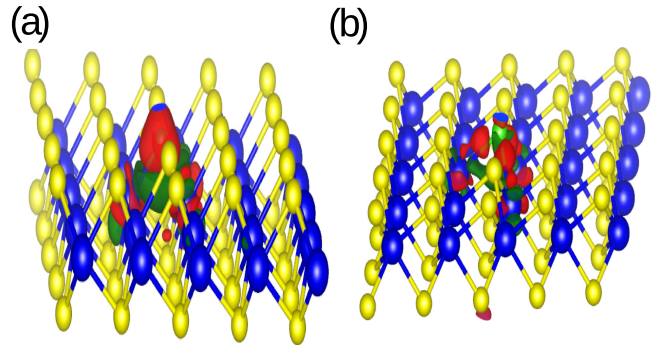


FIG. 6: (color online) Isosurface plots for electron density associated with Functionalized MoS₂ Monolayer with (a)F and (b)Cl. Red and green isosurface represents the charge accumulation and electron deficiency in the system. The blue and yellow balls represents Mo and S atoms in MoS₂ Monolayer.

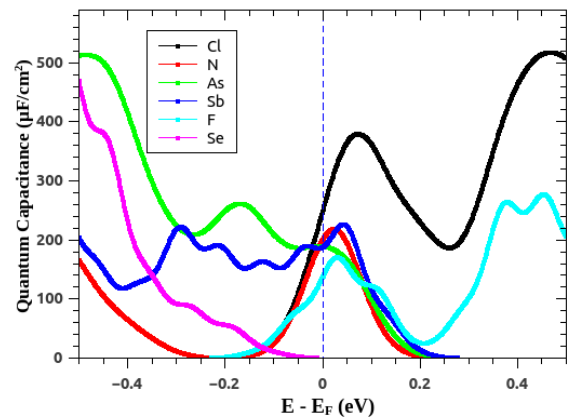


FIG. 7: (color online) The different color curve represents the energy variations of quantum capacitance for MoS₂ when S is substituted with various ad-atoms.

value occurs for V doped system $263 \mu\text{F}/\text{cm}^2$, whereas the quantum capacitance for other systems are also high

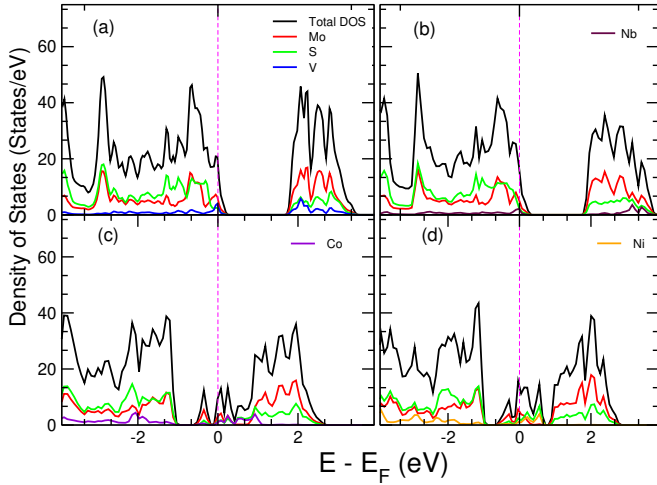


FIG. 8: (color online) Atom projected density of states for functionalized MoS₂ with (a)V, (b)Nb, (c)Co and (d)Ni atoms. Colored curve represents dos from the doped atom. Vertical majenta dashed line is the Fermi energy set at E=0.

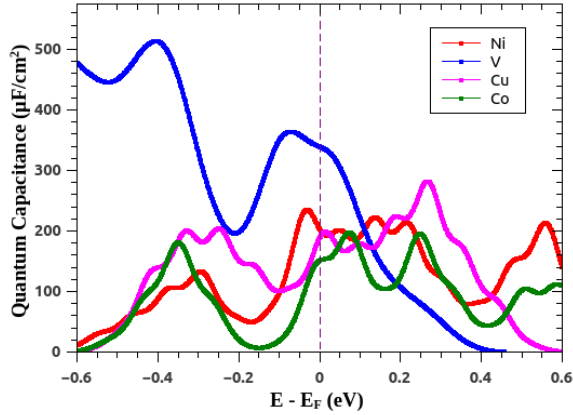


FIG. 9: (color online) The different color curve represents the energy variations of quantum capacitance for MoS₂ when Mo is substituted with various ad-atoms.

as listed in the TABLE.III. The energy variation of C_Q for each TM-doped systems are shown in Fig.9

TABLE III: Details of C_Q value calculated at Fermi energy for various ad-atom functionalized MoS₂.

Configuration	C_Q ($\mu\text{F}/\text{cm}^2$)	Configuration	C_Q ($\mu\text{F}/\text{cm}^2$)
FG - Co	152.794	FG - Ni	202.439
FG - Cu	191.658	FG - V	263.721

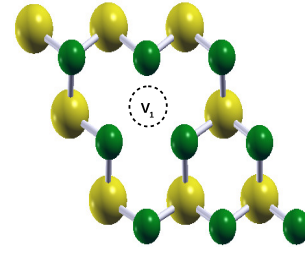


FIG. 10: (color online) Mo-vacancy defected MoS₂ structure. Green and yellow ball represents S and Mo atoms respectively.

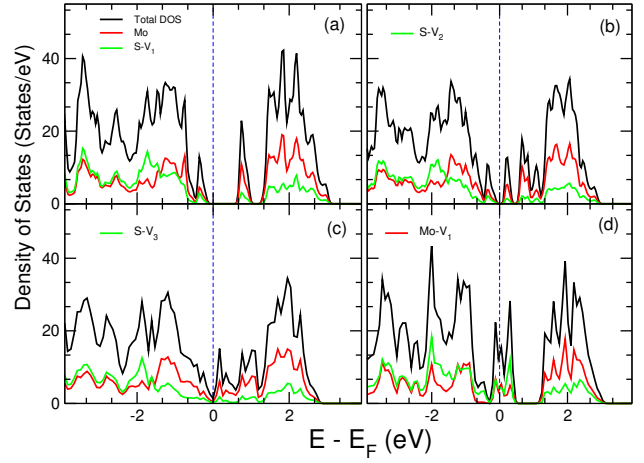


FIG. 11: (color online) Atom projected density of states for MoS₂ Monolayer with (a)One sulfur vacancy, (b)two sulfur vacancy, (c)three sulfur vacancy, (d)one Mo vacancy. Vertical blue dashed line is the Fermi energy set at E=0.

Impact of vacancy defects

Since the presence of vacancy defect can significantly alter the electronic structure of the materials, we, therefore, introduced a vacancy defect in monolayer MoS₂. The investigation has been carried out to understand the change in the electronic structure and subsequently the quantum capacitance of the system. Defected monolayer MoS₂ systems were modeled by removing a different number of S and Mo atoms from the 3×3 supercell. We have considered three different S vacancy concentrations by removing one, two, and three S atoms out of 18 S atoms in the unit cell respectively; ie with 5.5 %, 11%, and 16.5% S vacancy configurations. In the case of Mo vacancy, we could only investigate 11.5% vacancy defect configuration, as we found that the structure becomes unstable upon a further increment of the vacancy concentrations. Optimized unit cell structure of the Mo vacancy defected structure is shown in Fig.10

Our calculation shows that the sulfur vacancy in the

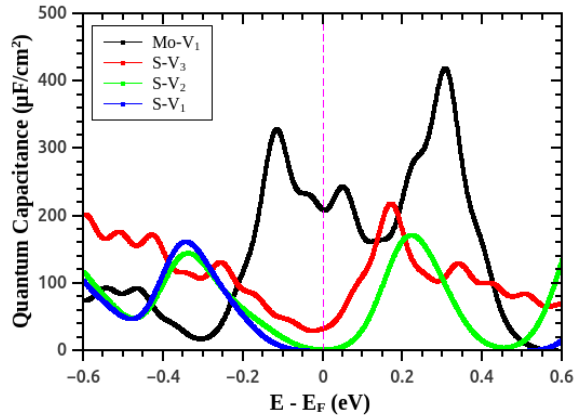


FIG. 12: (color online) The different color curve represents the energy variations of quantum capacitance for MoS₂ functionalized with various ad-atoms

system has a negligible impact on the value of C_Q . The maximum C_Q value obtained is $33 \mu\text{F}/\text{cm}^2$ for 16.5% defect configurations. However, in the case of 11% Mo vacancy defect system show a large quantum capacitance of $209.733 \mu\text{F}/\text{cm}^2$. The result can be analyzed from the obtained electronic structure of the defective system as shown in Fig.11. Mo-vacancy significantly changes the electronic structure and introduced a large amount of DOS near the Fermi energy and the system behaves as conductors. Whereas the change in DOS near the Fermi energy is negligible in the case of S-vacancy systems. The energy variation of C_Q for different configurations are shown in Fig.12 and the calculated quantum capacitances are listed in Table.IV.

TABLE IV: Details of C_Q value calculated at Fermi energy for various ad-atom functionalized MoS₂.

Configuration	C_Q ($\mu\text{F}/\text{cm}^2$)
MoS ₂ with 5.5% S vacancy	0.190
MoS ₂ with 11% S vacancy	2.500
MoS ₂ with 16.5% S vacancy	33.665
MoS ₂ with 11.5% Mo vacancy	209.733

CONCLUSION

In conclusion, we have studied the quantum capacitance in functionalized MoS₂ monolayer. Our theoretical investigation shows that the quantum capacitance (C_Q) of MoS₂ electrodes can be enhanced significantly by introducing ad-atoms and vacancy defects in the MoS₂ monolayer sheet. A marked quantum capacitance above $200 \mu\text{F}/\text{cm}^2$ has been observed. These calculations show that the quantum capacitance of MoS₂ monolayer enhances with substitutional doping of Mo with transition metal adatoms. A significant charge transfer and charge redistribution occur in ad-atom doped MoS₂ monolayer results in an accumulation of a large number of electronic states near Fermi level. The additional charge carriers brought by ad-atoms change the carrier concentration in monolayer MoS₂ that leads to the shift of the Fermi level and significantly improves the quantum capacitance of the system.

REFERENCES

- [1] Xu Q, Yang G, Fan X and Zheng W 2019 *Physical Chemistry Chemical Physics* **21** 4276–4285
- [2] Simon P and Gogotsi Y 2010 *Nanoscience and technology: a collection of reviews from Nature journals* 320–329
- [3] Wang G, Zhang L and Zhang J 2012 *Chemical Society Reviews* **41** 797–828
- [4] Huang X, Qi X, Boey F and Zhang H 2012 *Chemical Society Reviews* **41** 666–686
- [5] Hirunsit P, Liangruksa M and Khanchaitit P 2016 *Carbon* **108** 7–20
- [6] Choi B G, Hong J, Hong W H, Hammond P T and Park H 2011 *ACS nano* **5** 7205–7213
- [7] Stoller M D, Park S, Zhu Y, An J and Ruoff R S 2008 *Nano letters* **8** 3498–3502
- [8] Zhu Y, Murali S, Stoller M D, Ganesh K, Cai W, Ferreira P J, Pirkle A, Wallace R M, Cychosz K A, Thommes M et al. 2011 *science* **332** 1537–1541
- [9] Yang X, Cheng C, Wang Y, Qiu L and Li D 2013 *science* **341** 534–537
- [10] Kim T Y, Lee H W, Stoller M, Dreyer D R, Bielawski C W, Ruoff R S and Suh K S 2011 *ACS nano* **5** 436–442
- [11] Reina A, Jia X, Ho J, Nezich D, Son H, Bulovic V, Dreselhaus M S and Kong J 2009 *Nano letters* **9** 30–35
- [12] Kosynkin D V, Higginbotham A L, Sinitskii A, Lomeda J R, Dimiev A, Price B K and Tour J M 2009 *Nature* **458** 872–876
- [13] Merki D and Hu X 2011 *Energy & Environmental Science* **4** 3878–3888
- [14] Chang K and Chen W 2011 *Chemical Communications* **47** 4252–4254
- [15] Li Y, Wang H, Xie L, Liang Y, Hong G and Dai H 2011 *Journal of the American Chemical Society* **133** 7296–7299
- [16] Yin Z, Li H, Li H, Jiang L, Shi Y, Sun Y, Lu G, Zhang Q, Chen X and Zhang H 2012 *ACS nano* **6** 74–80
- [17] Bromley R, Murray R and Yoffe A 1972 *Journal of Physics C: Solid State Physics* **5** 759
- [18] Ramakrishna Matte H, Gomathi A, Manna A K, Late D J, Datta R, Pati S K and Rao C 2010 *Angewandte Chemie International Edition* **49** 4059–4062
- [19] Chodankar N, Nanjundan A, Losic D, Dubal D and Baek J B 2020 *Materials Today Advances* **6** 100053

- [20] Hwang H, Kim H and Cho J 2011 *Nano letters* **11** 4826–4830
- [21] Lin Y C, Dumcenco D O, Huang Y S and Suenaga K 2014 *Nature nanotechnology* **9** 391–396
- [22] Wang L, Xu Z, Wang W and Bai X 2014 *Journal of the American Chemical Society* **136** 6693–6697
- [23] Soon J M and Loh K P 2007 *Electrochemical and Solid State Letters* **10** A250
- [24] Ma G, Peng H, Mu J, Huang H, Zhou X and Lei Z 2013 *Journal of Power Sources* **229** 72–78
- [25] Xu Q, Yang G, Fan X and Zheng W 2019 *ACS omega* **4** 13209–13217
- [26] Sruthi T and Kartick T 2019 *Journal of Physics: Condensed Matter* **31** 475502
- [27] Kresse G and Furthmüller J 1996 *Physical review B* **54** 11169
- [28] Kresse G and Furthmüller J 1996 *Computational materials science* **6** 15–50
- [29] Perdew J P, Burke K and Ernzerhof M 1996 *Physical review letters* **77** 3865
- [30] Feng L p, Sun H q, Li A, Su J, Zhang Y and Liu Z t 2018 *Materials Chemistry and Physics* **209** 146–151
- [31] Mousavi-Khoshdel M, Targholi E and Momeni M J 2015 *The Journal of Physical Chemistry C* **119** 26290–26295
- [32] Mak K F, Lee C, Hone J, Shan J and Heinz T F 2010 *Physical review letters* **105** 136805